

Recovery of reactive MgO from reject brine via the addition of NaOH

Dong, Haoliang; Unluer, Cise; Yang, En-Hua; Al-Tabbaa, Abir

2018

Dong, H., Unluer, C., Yang, E. H., & Al-Tabbaa, A. (2018). Recovery of reactive MgO from reject brine via the addition of NaOH. *Desalination*, 42988-95.

<https://hdl.handle.net/10356/85818>

<https://doi.org/10.1016/j.desal.2017.12.021>

© 2017 Elsevier. This is the author created version of a work that has been peer reviewed and accepted for publication by *Desalination*, Elsevier. It incorporates referee's comments but changes resulting from the publishing process, such as copyediting, structural formatting, may not be reflected in this document. The published version is available at: [<http://dx.doi.org/10.1016/j.desal.2017.12.021>].

Downloaded on 20 Mar 2024 20:23:38 SGT

Cite as: H. Dong, C. Unluer, E.-H. Yang, A. Al-Tabbaa, Recovery of reactive MgO from reject brine via the addition of NaOH, Desalination (2018), 429, 88-95

Link: <https://doi.org/10.1016/j.desal.2017.12.021>

Recovery of reactive MgO from reject brine via the addition of NaOH

Haoliang Dong^a, Cise Unluer^a, En-Hua Yang^{a,*}, Abir Al-Tabbaa^b

^a School of Civil and Environmental Engineering, Nanyang Technological University, 50 Nanyang Avenue, Singapore 639798, Singapore

^b Department of Engineering, University of Cambridge, Trumpington Street, Cambridge CB2 1PZ, UK

Abstract

Reject brine, generated as a waste at the end of the desalination process, presents a useful source for the extraction of valuable resources. This study investigated the recovery of reactive MgO from reject brine obtained from a local desalination plant. This was enabled via the reaction of Mg^{2+} present within reject brine with an alkali source (NaOH), which led to the precipitation of $Mg(OH)_2$, along with a small amount of $CaCO_3$. The determination of the optimum NaOH/ Mg^{2+} ratio led to the production of the highest amount of yield. The synthesized $Mg(OH)_2$ was further calcined under a range of temperatures (500-700 °C) and durations (2-12 hours) to produce reactive MgO. A detailed characterization of MgO obtained under these conditions was presented in terms of its reactivity, specific surface area (SSA), composition and microstructure. While an increase in the calcination temperature and duration decreased the reactivity and SSA of MgO, samples calcined at 500 °C for 2 hours revealed the highest reactivity, which was reflected by their SSA of 51.4 m²/g.

Keywords: Reject brine; reactive MgO; NaOH; $Mg(OH)_2$; calcination

* Corresponding author. Address: N1-01b-56, 50 Nanyang Avenue, Singapore 639798. Tel.: +65 6790 5291; fax: +65 6791 0676. E-mail: ehyang@ntu.edu.sg

1 Introduction

Magnesium oxide (MgO) finds use in various applications ranging from the refractory industry to agriculture, chemical and environmental applications [1-4]. Another increasingly popular use of reactive MgO was reported in the construction industry as an expansive additive [5] and as a novel binder in the development of concrete formulations [6-11]. While the majority of MgO produced today is obtained through the processing of naturally occurring minerals such as magnesite (MgCO_3) [3], around 14% of the global MgO supply is from the calcination of magnesium hydroxide ($\text{Mg}(\text{OH})_2$) synthesized from seawater or magnesium-rich brine sources. The synthetic MgO obtained from seawater/brine demonstrates a higher purity and reactivity compared with MgO produced through the calcination of magnesite [12]. MgO that possesses higher purity and specific surface area (SSA) is widely used in high-end pharmaceutical and semiconductor applications as an additive or a catalyst [1-4].

The recovery of brucite ($\text{Mg}(\text{OH})_2$) from seawater/brine deploys the use of a strong base to precipitate Mg^{2+} from the solution. During this process, it is essential to reach an appropriate pH level in order to form the precipitates. Previous studies [13, 14] have shown that the ideal pH for the formation of carbonates is above 9, which favors the transformation of carbon dioxide and bicarbonates to CO_3^{2-} . The pH level of gelatinous $\text{Mg}(\text{OH})_2$ could be even higher due to the requirement of surplus hydroxide. These trends were also confirmed by [15], who demonstrated the occurrence of the precipitation process at a pH of 8.5, whereas higher pH values led to increased brucite formation.

Lime (CaO) [16] or dolomite lime ($\text{CaO}\cdot\text{MgO}$) [17] are used as a base during the synthesis of $\text{Mg}(\text{OH})_2$ from seawater. The use of dolomite lime reduces the amount of seawater/brine

needed for the production of the same amount of MgO obtained via the use of CaO because dolomite lime itself contains MgO. However, the uses of these Ca-bearing bases often lead to the precipitation of Ca-based compounds (e.g. CaCO_3) and thus reduce the purity and content of Mg-based precipitates. Furthermore, the Ca-bearing bases can react with sulphate (SO_4^{2-}) present in the solution to form gypsum ($\text{CaSO}_4 \cdot 2\text{H}_2\text{O}$), which may necessitate the pre-treatment of the solution through the addition of CaCl_2 to remove sulphate in seawater/brine.

Apart from Ca-based bases, several studies have suggested the use of other alkali sources to precipitate Mg^{2+} from seawater/brine [15, 18-23]. NaCO_3 and NaOH were reported to recover Ca and Mg from mining and seawater desalination brines. Recovery ratios higher than 94-96 % of Ca were achieved for pH higher than 10 via the use of NaCO_3 and recovery ratios higher than 97-99 % of Mg were achieved for pH higher than 11 via the addition of NaOH [23]. Another proposed additives was sodium hydroxide (NaOH) along with oxalic acid, which produce magnesium oxalate (MgC_2O_4) from brine. Previous studies [21] demonstrated the selective precipitation of Mg- and Ca-oxalate at different pH values. Ca-oxalate was first precipitated and removed at an oxalate/Ca molar ratio of 6.82 at a pH of < 1 . This was followed by the precipitation of Mg^{2+} from the brine residue at a $\text{NaOH}/\text{oxalate}/\text{Mg}$ ratio of 3.21:1:1.62 at a pH range of 3-5.5, leading to a high yield of pure magnesium oxalate.

These steps can be followed by the production of reactive MgO via the calcination of Mg-containing precipitates, such as magnesium hydroxide and magnesium oxalate. Numerous studies have been carried out to characterize MgO obtained from different sources [12, 24-32]. The outcomes of these studies have identified the main factors that influence the properties of MgO produced through the dry route (i.e. decomposition of magnesite) as the calcination conditions (i.e. temperature and residence time). Accordingly, increased

calcination temperatures and/or prolonged durations lead to the agglomeration of MgO particles due to sintering, which decreases the porosity and reactivity of MgO [30].

Desalination provides an alternative means to meet the residential and industrial water demands in water-stressed countries like Singapore [33, 34]. Currently, the two desalination plants in Singapore provide 100 million gallons (448,500 m³) of drinking water on a daily basis, which can meet 25% of Singapore's current water demand. With three additional desalination plants being built, the five desalination plants are designed to provide a total of 190 million gallons (852,150 m³) of water per day by 2020 [35]. On a global level, the daily production level of desalinated water by 18,426 desalination plants exceeds 86.8 million cubic meters [36]. Production of desalinated water generates an almost equal amount of reject brine [20], a high salt concentration waste by-product produced at the end of the desalination process [37]. Reject brine is often discharged directly back into sea, which threatens the marine life and ecosystem by altering the local flora and fauna due to its high salinity [38]. Therefore, the disposal and management of reject brine remains a major challenge as well as an environmental threat [38, 39], which can pave the way for its use in the recovery of valuable metals and useful solids instead of direct discharge [40].

The desalination process involves the addition of a variety of chemicals to enable the precipitation of the colloidal particles before running through the filtration process. Therefore, the resulting reject brine contains a very high concentration of dissolved salts and suspended constituents, creating variations in its composition in comparison to seawater, natural brine or synthetic solutions. While previous studies [15, 18-22] have reported the synthesis of MgO or its derivatives from seawater, natural brine or synthetic solutions, this study aims to explore the feasibility of the recovery of Mg²⁺ from reject brine collected from

a local desalination plant. The proposed method involves the addition of NaOH, which serves as a pH adjuster and controls the pH of the solution. Unlike Ca-bearing bases, which often lead to the precipitation of a Ca-based compound (e.g. CaCO_3) along with Mg-phases, the use of NaOH can increase the purity of Mg-based precipitates. Furthermore, when compared with other bases (e.g. NH_4OH , KOH and Na_2CO_3), NaOH possesses other advantages in terms of health and safety, cost effectiveness and base strength it provides [31].

This research presents a comprehensive study on the synthesis of $\text{Mg}(\text{OH})_2$ and production of reactive MgO from reject brine via the use of NaOH. The key parameters affecting the properties of the synthesized $\text{Mg}(\text{OH})_2$ and its calcination to produce reactive MgO were investigated. Several techniques were utilized to characterize the synthesized $\text{Mg}(\text{OH})_2$ and MgO including inductively coupled plasma-optical emission spectroscopy (ICP-OES), X-ray powder diffraction (XRD), field emission scanning electron microscopy (FESEM), thermogravimetric and differential thermal analysis (TG/DTA), Brunauer-Emmett-Teller (BET) analysis and acid neutralization. Production cost of reactive MgO from reject brine via the addition of NaOH was calculated to evaluate the economic feasibility of the approach. Results obtained at the end of this study were used to demonstrate the use of reject brine as an alternative source for the recovery of MgO with a high reactivity.

2 Materials and Methodology

2.1 Materials

Reject brine was collected and sampled from a local desalination plant in Singapore, which adopts a reverse osmosis (RO) membrane system to purify saline water and produce drinkable water for human use. These membranes reject more than 99.5% of the dissolved

salts and suspended materials in the feedwater, resulting in a highly concentrated reject waste stream which contains suspended constituents and a 2- to 7-fold increased concentration of dissolved salts [33, 34, 41]. Prior to any analysis, the reject brine was first filtrated through a 45 μm membrane filter to remove the large suspended solids. The pH of reject brine as received was around 8.0. The chemical composition of the reject brine, obtained via inductively coupled plasma-optical emission spectroscopy (ICP-OES) and ion chromatography (IC), is summarized in Table 1. Along with Mg^{2+} , which was present at a concentration of 1718 ppm, other impurities such as Na^+ , K^+ and Ca^{2+} were also identified in the reject brine. Sodium hydroxide (NaOH, reagent grade, pellets) supplied by VWR Pte Ltd in Singapore, was used as the alkaline base in the current study.

Table 1 Chemical composition of the reject brine used in this study

Element	Cl	Na	SO_4	Mg	K	Ca	Sr	B	Si	Li	P	Al
Concentration (ppm)	55243	13580	4423	1718	845.7	471.3	14.6	3.8	3.7	0.3	0.2	0.1

2.2 Methodology

Different amounts of NaOH solution (16 M) were added into 200 ml of reject brine to study the influence of NaOH/ Mg^{2+} molar ratio (ranging from 2 to 4) on the recovery of Mg^{2+} . NaOH solution was added into reject brine at once and the initial pH of solution was recorded. The solution was mixed at constant speed of 300 rpm by a magnetic stirrer at room temperature (25 $^{\circ}\text{C}$). A pH/thermometer probe was used to monitor and record the temperature and pH of the reaction in the solution. Experiment was terminated when the pH of the solution stabilized. The solids were separated from the residual brine through a centrifuge. After the solids were collected, they were re-dispersed and washed thoroughly by ultra-pure water in an ultrasonic bath to remove surface-attached ions. The washed solids were separated from the solution through a centrifuge. This washing process was repeated for

three times to remove surface-attached ions and soluble salts. The washed solids were then oven-dried at 105 °C for 24 hours to remove free water before grinding into powder form. The ground samples were calcined at pre-determined temperatures (500-700 °C) and durations (2-12 hours) in an electric furnace to produce reactive MgO.

Several techniques were utilized to characterize the synthesized $\text{Mg}(\text{OH})_2$ and MgO. X-ray powder diffraction (XRD) was performed via a Bruker D8 Advance with a Cu $K\alpha$ source under the operation conditions of 40 kV and 40 mA, emitting radiation with a wavelength of 1.5405 angstroms, scan rate of 0.02 °/step, and a 2θ range of 5 to 70°. A JSM-7600F thermal field emission scanning electron microscopy (FESEM) was used to analyze the microstructure of the solids by imaging powder surface. The decomposition of each sample was studied via thermogravimetric and differential thermal analysis (TG/DTA) using a PyrisDiamond TGA 4000 operated at a heating rate of 10 °C/min under air flow. The specific surface area (SSA) of the synthesized samples was obtained by Brunauer-Emmett-Teller (BET) analysis from nitrogen adsorption-desorption isotherms using a Quadrasorb Evo automated surface area and pore size analyser. The reactivity of MgO was measured by acid neutralization, during which 0.28 grams of the synthesized MgO was added into 50 ml of 0.07 mol/L citric acid solution along with phenolphthalein (i.e. pH indicator). The neutralization time was measured and reported as an indicator of reactivity [3, 30].

Economic feasibility of the production of reactive MgO from reject brine in this study was evaluated and compared with other production routes. The total cost of the production of reactive MgO from reject brine mainly consists of the raw material cost for synthesis (e.g. NaOH) and the energy cost during calcination. Reject brine is the waste water produced at the end in the desalination plant, and thus the material cost and energy cost of reject brine are

assumed to be zero. Transportation of raw materials and the grinding and packing of reactive MgO products are not considered into the calculation since they do not contribute significantly to the overall process.

3 Results and Discussion

3.1 Recovery of Mg^{2+} and Ca^{2+} from reject brine

The formation of $Mg(OH)_2$ was observed via the reaction between the Mg^{2+} in the reject brine and OH^- provided by NaOH. The addition of NaOH also enabled the conversion of HCO_3^- , present in the reject brine, to CO_3^{2-} . This led to a reaction of CO_3^{2-} with Ca^{2+} and resulted in the precipitation of $CaCO_3$. The reaction paths observed during this process are shown in Equations 1-4 below.



The kinetics of the reaction between reject brine and NaOH reflected by the change of pH are summarized in Figure 1. A rapid reaction was observed, which was completed in less than 30 minutes as the pH reached an equilibrium state. The pH increased with the molar ratio of NaOH/ Mg^{2+} . This was due to the increased concentration of OH^- provided by the higher amounts of NaOH introduced into the solution, whereas a smaller increase was observed at NaOH/ Mg^{2+} ratios of > 2.5 .

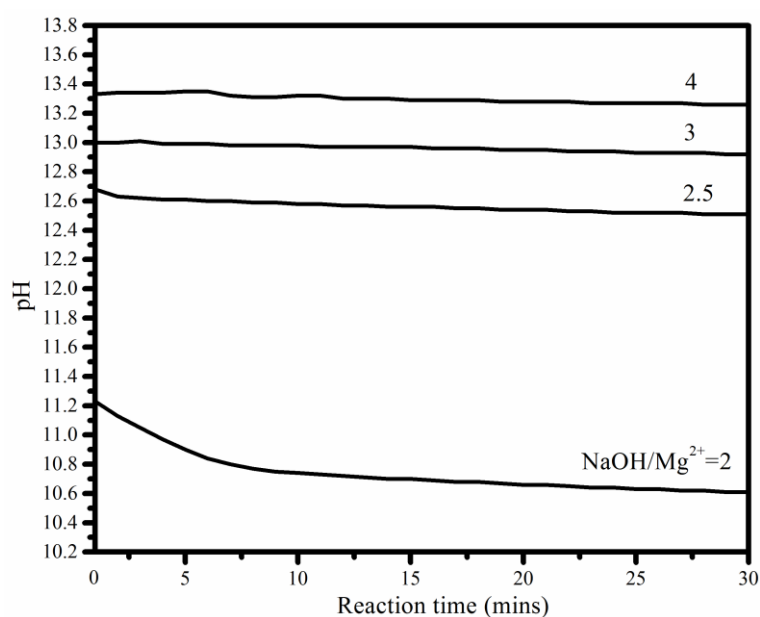
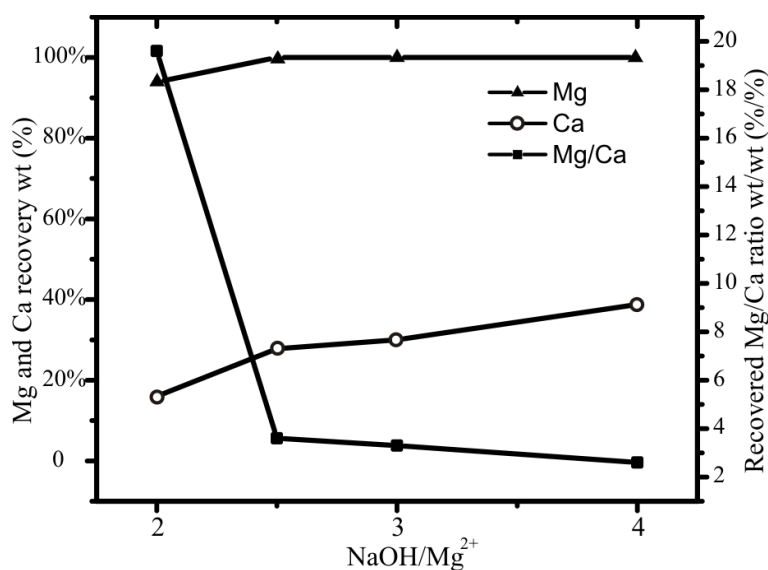


Figure 1 pH of the reaction between reject brine and NaOH at different NaOH/Mg²⁺ ratios

Figure 2 shows the recovery rate of Mg²⁺ and Ca²⁺ in weight percentage after the reaction of reject brine with NaOH. As can be seen, the recovery rates for both Mg²⁺ and Ca²⁺ increased with increasing NaOH/Mg²⁺ molar ratio, which achieved a similar recovery level of 94-99% of Mg as reported in [23]. The recovered Mg²⁺/Ca²⁺ ratio was used as an indication of the purity level of the resulting Mg(OH)₂ precipitates. As shown in Figure 2, Mg²⁺/Ca²⁺ was highest (19.6) at a NaOH/Mg²⁺ ratio of 2 and decreased with increasing NaOH/Mg²⁺ ratio. This was because at a NaOH/Mg²⁺ molar ratio of 2, the ion product in the solution ($[Mg^{2+}][OH^-]^2 = 7 \times 10^{-8.6} \text{ mol}^3 \text{ l}^{-3}$, pH = 11.2) was larger than the solubility product constant of Mg(OH)₂ ($1.8 \times 10^{-11} \text{ mol}^3 \text{ l}^{-3}$) [42]. The supersaturation condition enabled the reaction between OH⁻ and Mg²⁺ and the formation of Mg(OH)₂. Furthermore, pH increased with increasing NaOH/Mg²⁺, which provided excessive OH⁻ in the solution to attack HCO₃⁻. This caused in a shift in Equation 3 towards the right hand side, resulting in the generation of additional CO₃²⁻. The excessive CO₃²⁻ reacted with Ca²⁺ in the solution to produce more CaCO₃, thus lowering the overall Mg²⁺/Ca²⁺ ratio.

224



225

226 Figure 2 Percentage of Mg²⁺ and Ca²⁺ sequestered from reject brine as a function of the
227 NaOH/Mg²⁺ molar ratio

228

229 3.2 Characterization of the synthesized Mg(OH)₂

230

231 3.2.1 XRD

232 Figure 3 shows the XRD diffractograms of Mg(OH)₂ obtained from the reaction of reject
233 brine and NaOH at different NaOH/Mg²⁺ molar ratios. The diffraction patterns of all samples
234 demonstrated the presence of Mg(OH)₂ along with CaCO₃. A shift in the crystal structure of
235 CaCO₃ from aragonite to calcite was observed at increased NaOH/Mg²⁺ ratios. This could be
236 attributed to the presence of Mg²⁺ in brine, which inhibited the precipitation of calcite and
237 favored the formation of aragonite at low NaOH/Mg²⁺ ratios [43]. Alternatively, the high pH
238 of the solution at elevated NaOH/Mg²⁺ ratios, at which the influence of Mg²⁺ was minimal,
239 favored the formation of calcite.

240

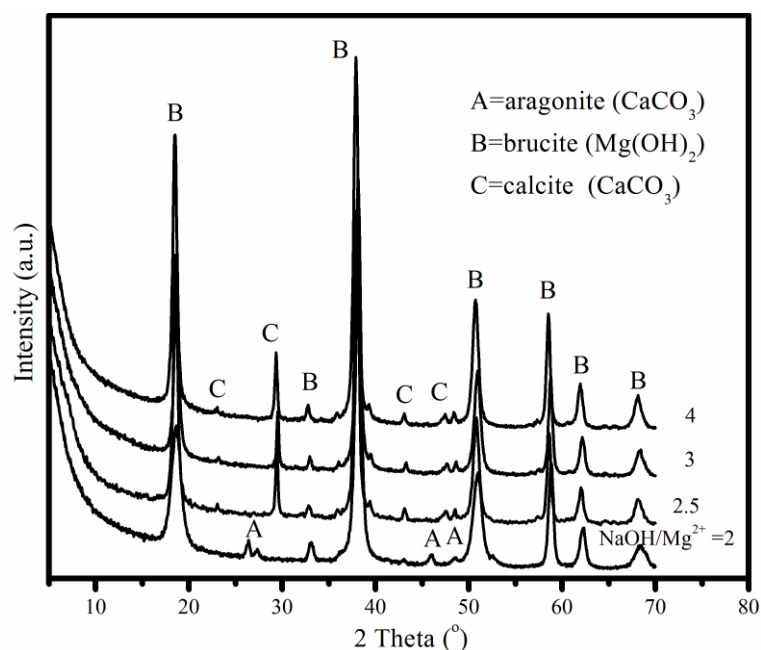


Figure 3 XRD diffractograms of $\text{Mg}(\text{OH})_2$ obtained from the reaction of reject brine with NaOH at different $\text{NaOH}/\text{Mg}^{2+}$ molar ratios

3.2.2 FESEM

The morphologies of $\text{Mg}(\text{OH})_2$ samples obtained at different $\text{NaOH}/\text{Mg}^{2+}$ molar ratios were investigated by FESEM, as shown in Figure 4. A plate-like morphology was observed at a $\text{NaOH}/\text{Mg}^{2+}$ ratio of 2. The morphology of $\text{Mg}(\text{OH})_2$ transformed into a granular pattern consisting of a denser structure at increased $\text{NaOH}/\text{Mg}^{2+}$ ratios, which could be due to the increased pH of the solution. This was because higher pH values led to the generation of higher concentrations of OH^- in the solution. The increased availability of OH^- accelerated the nucleation of $\text{Mg}(\text{OH})_2$ crystals and enabled the formation of larger amounts of $\text{Mg}(\text{OH})_2$, facilitating the densification of the overall structure.

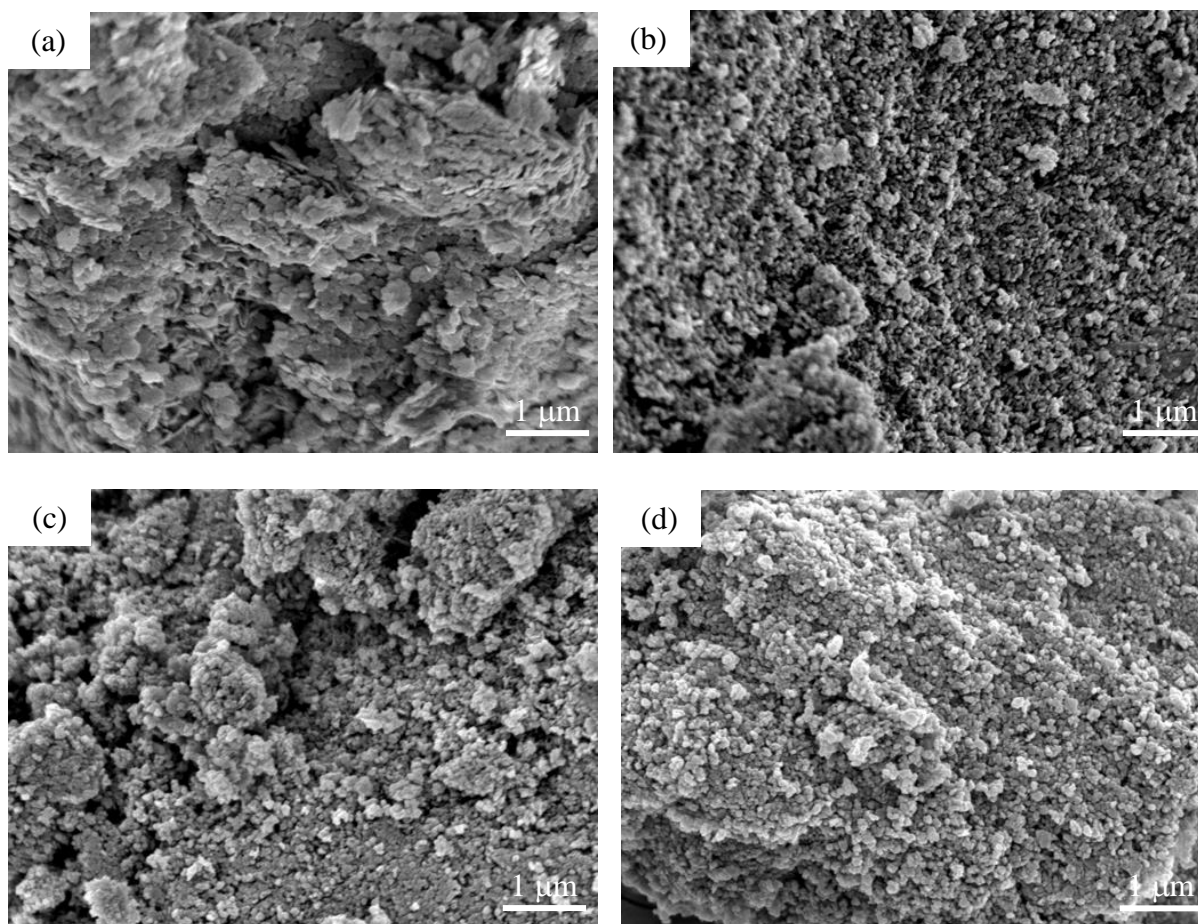


Figure 4 FESEM images of Mg(OH)₂ obtained from the reaction of reject brine with NaOH at different NaOH/Mg²⁺ molar ratios of (a) 2, (b) 2.5, (c) 3 and (d) 4

3.2.3 TG/DTA

Figure 5 illustrates a typical TG/DTA graph of Mg(OH)₂ obtained via the reaction of brine with NaOH at a NaOH/Mg²⁺ molar ratio of 2. The dehydration of Mg(OH)₂ took place at ~400 °C and resulted in a mass loss of around 24.2%, which was attributed to the loss of water. The decomposition patterns observed during TG/DTA were in line with previous studies that investigated the decomposition of Mg(OH)₂ into MgO [24, 26-28, 30, 32]. The second endothermic peak, observed at ~720 °C, was due to the decarbonation of CaCO₃. The decomposition of CaCO₃ led to the release of CO₂, resulting in a mass loss of around 2.3%.

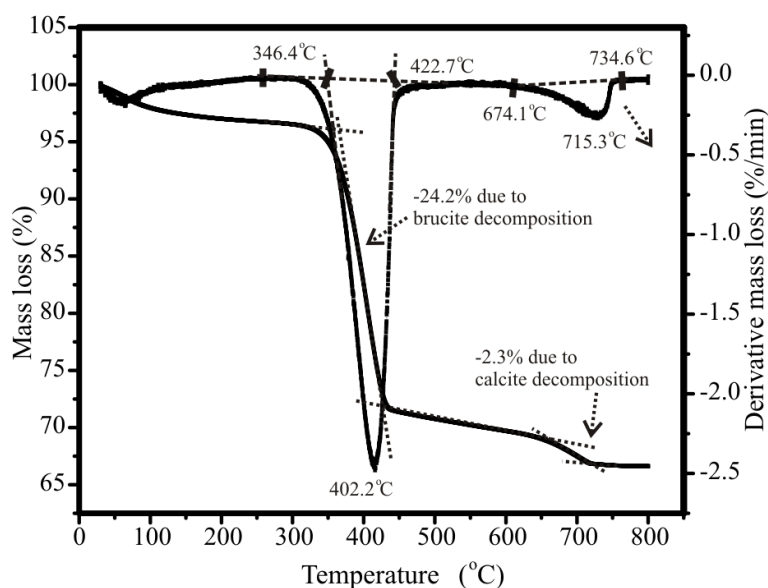


Figure 5 A typical TG/DTA curve of $\text{Mg}(\text{OH})_2$ obtained from the reaction of reject brine at a $\text{NaOH}/\text{Mg}^{2+}$ molar ratio of 2

Table 2 summarizes the TG/DTA results of $\text{Mg}(\text{OH})_2$ obtained from the reaction of brine with NaOH at various $\text{NaOH}/\text{Mg}^{2+}$ ratios ranging between 2 and 4. The results show that the mass loss due to dehydration of $\text{Mg}(\text{OH})_2$ at $\sim 400^\circ\text{C}$ slightly decreased (24.2 to 22.6%), while the mass loss due to decarbonation of CaCO_3 at $\sim 720^\circ\text{C}$ slightly increased (2.3 to 3.9%) with increasing $\text{NaOH}/\text{Mg}^{2+}$ ratios. This was mainly attributed to the increased content of CaCO_3 in the precipitates at higher $\text{NaOH}/\text{Mg}^{2+}$ ratios, which was in line with the findings shown in Figure 2.

Table 2 TG/DTA results of the decomposition of $\text{Mg}(\text{OH})_2$ obtained from the reaction of reject brine with NaOH at different $\text{NaOH}/\text{Mg}^{2+}$ ratios

$\text{Mg}^{2+}/\text{NaOH}$	Peak temperature ($^\circ\text{C}$)	Mass loss between 340-440 $^\circ\text{C}$ (%)	Peak temperature ($^\circ\text{C}$)	Mass loss between 650-750 $^\circ\text{C}$ (%)
1:2	402.2	24.2	715.3	2.3
1:2.5	401.2	23.5	721.1	3.2
1:3	400.8	23.3	719.3	3.5
1:4	404.1	22.6	724	3.9

Table 3 compares the compositions of the synthesized $\text{Mg}(\text{OH})_2$ based on the TG/DTA (Table 2) and the ICP-OES (Figure 2) results. Both measurements revealed similar trends, showing a decrease in the mass percentage of $\text{Mg}(\text{OH})_2$, accompanied with an increase in the mass percentage of CaCO_3 (and thus a decrease in the purity of precipitates) with increasing $\text{NaOH}/\text{Mg}^{2+}$ molar ratios, which was further discussed in Section 3.1. Accordingly, the highest amount of $\text{Mg}(\text{OH})_2$ (93.7% by TGA and 95.4% by ICP-OES) was synthesized at a $\text{NaOH}/\text{Mg}^{2+}$ molar ratio of 2. Therefore, this ratio was chosen as the optimum condition for the subsequent production and characterization of reactive MgO .

Table 3 Composition of synthesized $\text{Mg}(\text{OH})_2$ based on TG/DTA and ICP-OES results

$\text{Mg}^{2+}/\text{NaOH}$	TG/DTA		ICP-OES	
	$\text{Mg}(\text{OH})_2$ (%)	CaCO_3 (%)	$\text{Mg}(\text{OH})_2$ (%)	CaCO_3 (%)
1:2	93.7	6.3	95.4	4.6
1:2.5	91.2	8.8	91.2	8.8
1:3	90.4	9.6	90.6	9.4
1:4	89.2	10.8	88.1	11.9

3.3 Characterization of the synthesized reactive MgO

3.3.1 SSA

Figure 6 presents the SSA of the reactive MgO obtained under different calcination conditions. In general, SSA reduced with increasing calcination temperature and duration, which was in line with the findings of previous studies [24, 26-28, 30, 32]. This was associated with the sintering and agglomeration of MgO grains at higher temperature and prolonged residence times. In the current study, the highest SSA of $51.4 \text{ m}^2/\text{g}$ was obtained when the synthesized $\text{Mg}(\text{OH})_2$ was calcined at 500°C for 2 hours. When compared to other studies, the SSA value ($51.4 \text{ m}^2/\text{g}$) obtained under these conditions was significantly higher than the results presented in the literature, where MgO synthesized from a magnesium

chloride solution via the addition of NaOH and calcined under the same conditions (i.e. 500 °C for 2 hours), was reported to possess a SSA of 22.1 m²/g [44]. However, compared with our previous study, MgO calcined at 500 °C for 2 hours from reject brine via the addition of NH₄OH showed a higher SSA of 78.8 m²/g [31]. This could be because the use of NaOH as the alkali source was found to form Mg(OH)₂ with a globular cauliflower-like morphology; while the use of NH₄OH resulted in a more porous plate-like morphology [31]. A relative more porous mother precursor would result in a more porous MgO, thus a higher reactivity. These values can be optimized even further with an adjustment of the calcination temperature and duration towards the lower range, while enabling the complete decomposition of Mg(OH)₂.

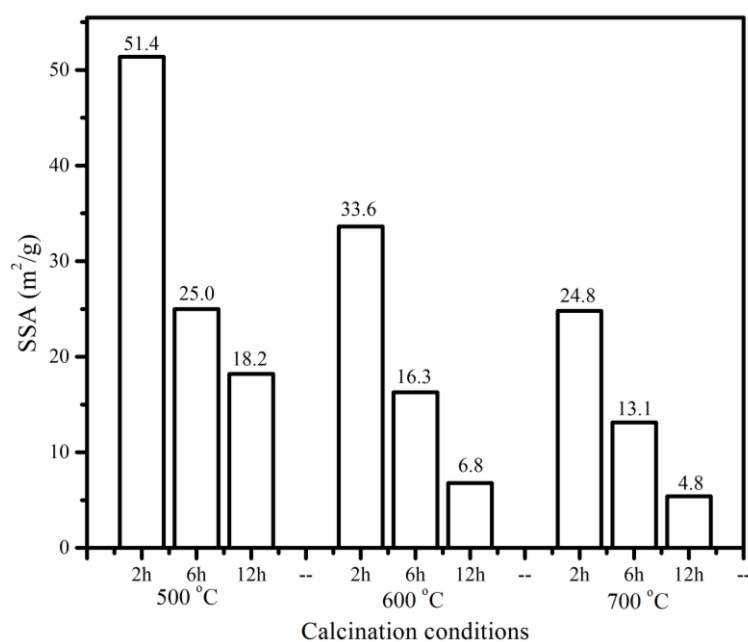


Figure 6 SSA of MgO produced under different calcination temperatures and durations

3.3.2 Reactivity

Figure 7 shows the acid reactivity of MgO obtained under different calcination conditions. An increase in the neutralization time was observed with increasing calcination temperature and

duration, which reflected the reduction in the reactivity of MgO. This observation corresponded well with the SSA measurements reported earlier in Figure 6. A comparison of the reactivity and SSA of MgO is shown in Figure 8, where the inverse correlation between the two parameters was revealed. Accordingly, MgO samples with higher SSA resulted in shorter acid neutralization times, which was an indication of their higher reactivities. These findings were in line with those reported in earlier studies [12, 30], where a direct correlation between the SSA and reactivity of MgO was reported.

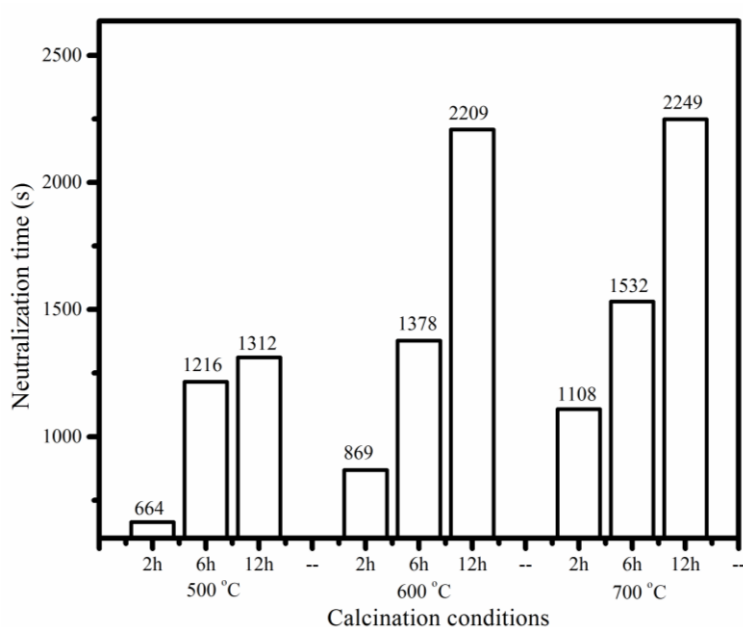


Figure 7 Effect of calcination temperature and duration on the reactivity of MgO

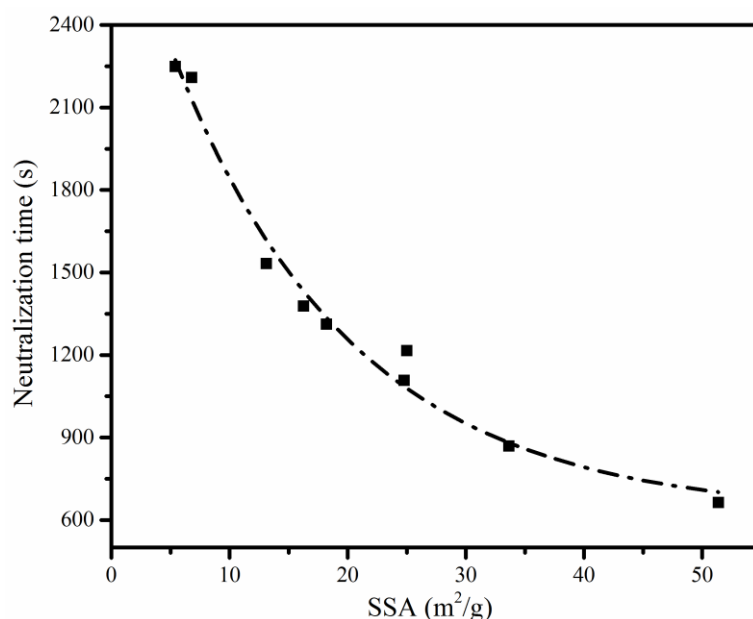


Figure 8 Relationship between the SSA and the reactivity of MgO

3.3.3 XRD

Figure 9 illustrates the diffractograms of MgO obtained via the calcination of Mg(OH)₂, which was synthesized at a NaOH/Mg²⁺ molar ratio of 2. The main peak positions of the synthesized MgO were located at ~37.0°, 42.9° and 62.3° 2θ, which matched well with the reference peaks of MgO indicated in JCPDS card no. 89-7746. These peaks were accompanied with a few minor peaks attributed to CaCO₃. The absence of Mg(OH)₂ peaks indicated the complete decomposition of brucite under the calcination conditions adopted in this study. Aragonite, which was initially present along with Mg(OH)₂, transformed into calcite at higher calcination temperatures of 600 °C [45]. A further increase in the calcination temperature (700 °C) and duration led to a reduction in the intensity of the calcite peaks due to decomposition of CaCO₃.

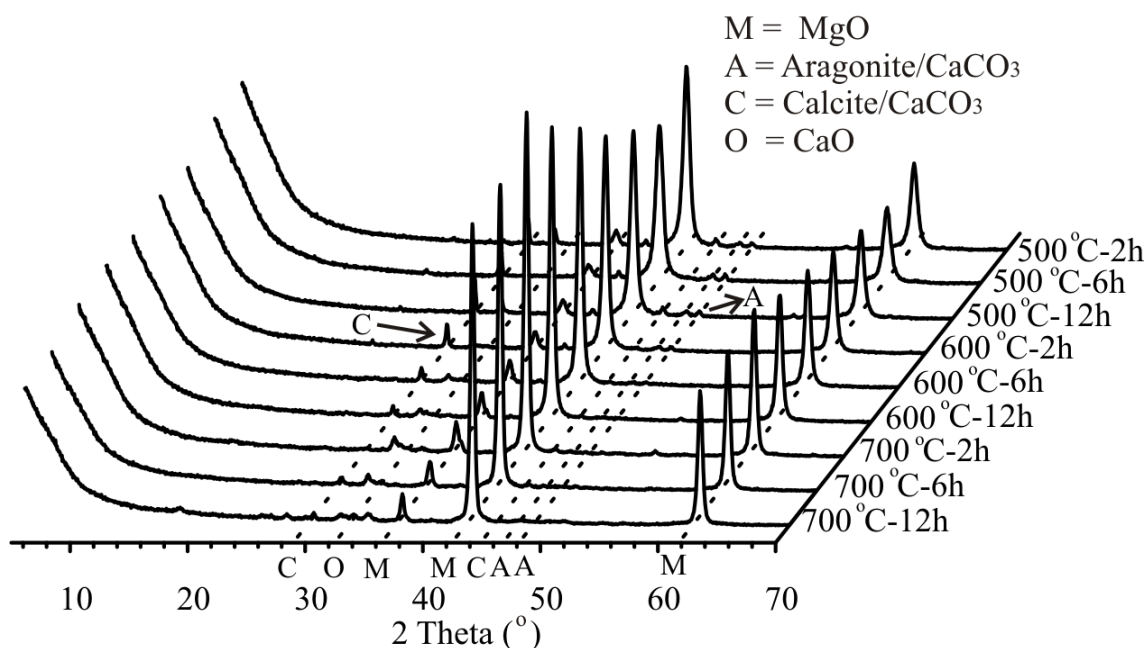


Figure 9 XRD diffractograms of reactive MgO produced via the calcination of $\text{Mg}(\text{OH})_2$ under different temperatures and durations

3.3.4 FESEM

A further investigation on the influence of calcination temperature and duration on the SSA of MgO was revealed through FESEM. The changes in the microstructure of MgO at increased temperatures and durations are indicated in Figure 10, which is a good indication of the typical morphology of MgO produced at a calcination temperature of 500-700 °C and a residence time of 2-12 hours. The microstructure of MgO was composed of a single particle which was a combination of several grains. A plate-like morphology, which was inherited from the parent material ($\text{Mg}(\text{OH})_2$), was observed throughout the microstructure of MgO produced at lower temperatures. An increase in the particle size, accompanied with the creation of a more porous structure, was observed at increased temperatures and durations. The loss of water during the decomposition of $\text{Mg}(\text{OH})_2$ led to the formation of a porous structure, which gradually reduced with the increase in the size of the MgO grains due to continued sintering, causing a reduction in the total pore volume.

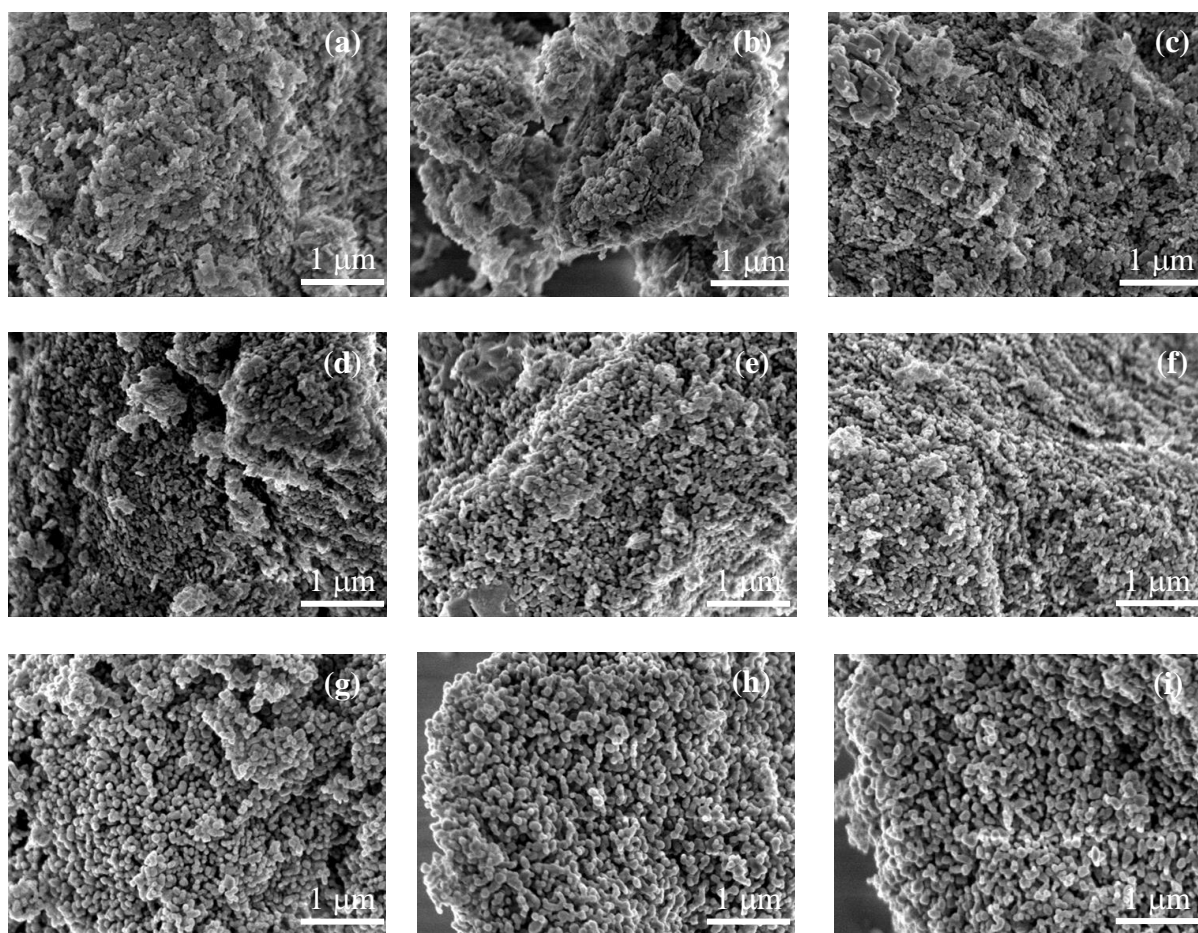


Figure 10 FESEM images of MgO obtained from the calcination of $\text{Mg}(\text{OH})_2$ under different conditions: (a) 500°C-2h, (b) 500°C-6h, (c) 500°C-12h, (d) 600°C-2h, (e) 600°C-6h, (f) 600°C-12h, (g) 700°C-2h, (h) 700°C-6h and (i) 700°C-12h

3.4 Economic feasibility

The costs of the production of reactive MgO from reject brine via the addition of NaOH, NH_3 , or CaO were calculated and compared. In the first step, base is added into reject brine to precipitate $\text{Mg}(\text{OH})_2$. Raw material costs of NaOH, NH_3 , and CaO are reported to be ~\$571/ton NaOH [46], ~\$525/ton NH_3 [47], and ~\$170/ton CaO [48], respectively. Cost of reject brine, transportation of raw materials, and grinding and packing of reactive MgO are not considered. Since a production yield of 1 ton reactive MgO requires 2 tons NaOH, 1 ton

NH₃, or 1.4 ton CaO as the base source, the raw material costs are calculated to be S\$1142/ton MgO, S\$525/ton MgO and S\$238/ton MgO via the addition of NaOH, NH₃, or CaO, respectively.

The resulting Mg(OH)₂ produced in the first step was in the form of filter cake which consists of 55.2% solids and 44.8% free water. In the second step, Mg(OH)₂ filter cake was calcinated to produce MgO. Energy consumption during calcination of Mg(OH)₂ filter cake is derived by considering the following two steps: (i) Energy consumed to increase the temperature from room temperature (298 K, 25 °C) to the decomposition temperature of Mg(OH)₂ (773K, 500 °C), and (ii) enthalpy of decomposition of Mg(OH)₂ [3]. A production yield of 1 ton MgO requires decomposing 1.45 ton Mg(OH)₂ and the decomposition temperature of Mg(OH)₂ under one atmosphere CO₂ pressure is in the range between 773 and 973 K (500 and 700 °C). Firstly the energy required to raise the temperature from ambient air (298 K) to the decomposition temperature (773 K) is calculated using the formula: $C_p \times \text{increase in temperature (K)}$. The specific heat capacity (C_p) of Mg(OH)₂ at 773 K is 1.78 kJ/kg K, which results in the energy demand of 1.15 GJ in consideration of the purity of the synthesized Mg(OH)₂ of ~94%. The energy required for decomposition of Mg(OH)₂ is calculated based on the enthalpy of decomposition (1304 kJ/kg K), which brings in 1.77 GJ. As for the free water, energy required to increase temperature of free water from room temperature (298 K) to the boiling point (373 K) is calculated based on the specific heat capacity of water (4.18 kJ/kg K) and the percentage of water in the filter cake (44.8%), resulting in 0.37 GJ. This is followed by the enthalpy of the vaporization of water (2283 kJ/kg K), resulting in 2.69 GJ. Finally the energy required to heat up the resultant steam to 773 K is calculated via the heat capacity of water vapour (1.86 kJ/kg K), bringing in 0.88 GJ. The total energy required for the calcination process is the summation of the energy required for each individual step,

resulting in a total of 6.85 GJ (1902.8 kWh) for the production of 1 ton reactive MgO from reject brine via the addition of base. As of 2015, Singapore uses natural gas (95%) and others (4%) for the power generation at a price of 20.2 cents per kWh [49], which results in an energy cost of S\$384 to product 1 ton reactive MgO from reject brine via the addition of a base.

Production cost of the resulting MgO via the addition of NaOH, NH₃, and CaO in reject brine are S\$1526, S\$909, and S\$622 per ton MgO, respectively, as shown in Figure 11. Price of MgO produced via a dry route in the US market was reported to be S\$617 per ton MgO [50]. Thus, a cheaper base alternative would make the production of reactive MgO from reject brine more economically feasible. Furthermore, synthetic MgO from reject brine shows a much higher purity and reactivity compared to the dry route as the SSA of commercial MgO is usually ~20 m²/g [3], which makes synthetic MgO more competitive in the global market.

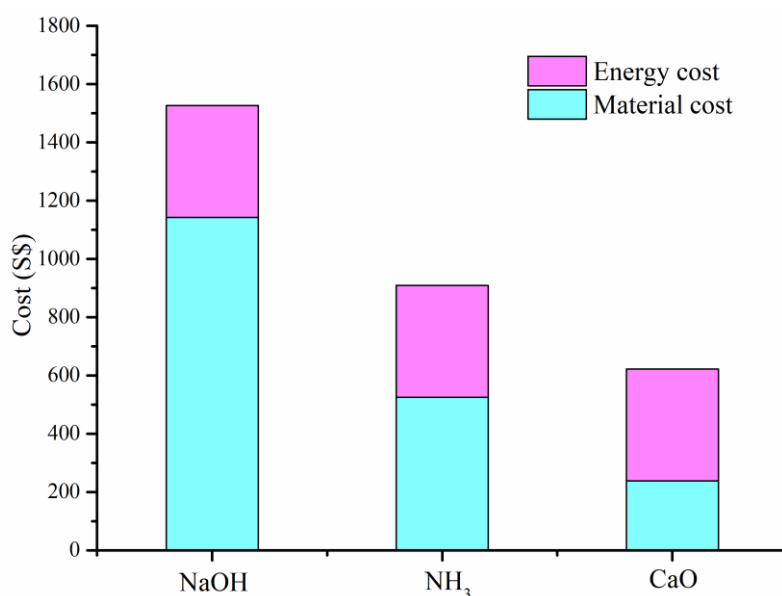


Figure 11 Production cost of reactive MgO from reject brine via the addition of NaOH, NH₃, or CaO.

4 Conclusions

This study presented a comprehensive investigation on the synthesis of $\text{Mg}(\text{OH})_2$ and production of reactive MgO from reject brine via the use of NaOH . The key parameters affecting the properties of the synthesized $\text{Mg}(\text{OH})_2$ and its calcination to produce reactive MgO were revealed. The results demonstrated the feasibility of recovering reactive MgO from reject brine obtained as a waste at the end of the desalination process. The initial set of experiments successfully demonstrated the use of NaOH as an alkali source in the precipitation of $\text{Mg}(\text{OH})_2$ from reject brine. The effect of the $\text{NaOH}/\text{Mg}^{2+}$ ratio on the final yield was investigated with the goal of optimizing the amount and purity of the synthesized $\text{Mg}(\text{OH})_2$. An optimum $\text{NaOH}/\text{Mg}^{2+}$ ratio of 2, which generated the highest purity of $\text{Mg}(\text{OH})_2$, was determined and used in the subsequent production of MgO . The influence of calcination conditions (i.e. temperature and residence time) on the reactivity of MgO obtained via the calcination of the synthesized $\text{Mg}(\text{OH})_2$ were reported. While a certain minimum temperature was required for the complete decomposition of $\text{Mg}(\text{OH})_2$ into MgO , an increase in the calcination temperature and duration lowered the reactivity of MgO . Calcination of $\text{Mg}(\text{OH})_2$ at $500\text{ }^\circ\text{C}$ for 2 hours resulted in the most reactive MgO samples, with a SSA of $51.4\text{ m}^2/\text{g}$. This study demonstrated that reject brine can be considered as a feasible and economic alternative source for the sustainable recovery of MgO with a high reactivity, which can be used in various applications within the food, cosmetics, pharmaceutical and construction industries [1-3].

Acknowledgement

This project is funded by the National Research Foundation (NRF), Prime Minister's Office, Singapore under its Campus for Research Excellence and Technological Enterprise (CREATE) program. Special thanks to Ms. Rui Hao for her review and comments of the

449 manuscript.

450

451

References

- [1] D.A. Kramer, Magnesium, its alloys and compounds, Industrial Minerals and Rocks, 2001.
- [2] E.K. Lee, K.D. Jung, O.S. Joo, Y.G. Shul, Magnesium oxide as an effective catalyst in catalytic wet oxidation of H₂S to sulfur, Reaction Kinetics and Catalysis Letters, 82, 2004, 241-246.
- [3] M.A. Shand, The chemistry and technology of magnesia, 2006.
- [4] M.A. Caraballo, T.S. Rotting, F. Macias, J.M. Nieto, C. Ayora, Field multi-step limestone and MgO passive system to treat acid mine drainage with high metal concentrations, Applied Geochemistry, 24, 2009, 2301-2311.
- [5] L.W. Mo, M. Deng, M.S. Tang, A. Al-Tabbaa, MgO expansive cement and concrete in China: Past, present and future, Cement and Concrete Research, 57, 2014, 1-12.
- [6] A.J.W. Harrison, Reactive magnesium oxide cements, 2008.
- [7] M. Liska, A. Al-Tabbaa, K. Carter, J. Fifield, Scaled-up commercial production of reactive magnesium cement pressed masonry units. Part I: Production, Proceedings of the Institution of Civil Engineers-Construction Materials, 165, 2012a, 211-223.
- [8] M. Liska, A. Al-Tabbaa, K. Carter, J. Fifield, Scaled-up commercial production of reactive magnesia cement pressed masonry units. Part II: Performance, Proceedings of the Institution of Civil Engineers-Construction Materials, 165, 2012b, 225-243.
- [9] C. Unluer, A. Al-Tabbaa, Impact of hydrated magnesium carbonate additives on the carbonation of reactive MgO cements, Cement and Concrete Research, 54, 2013, 87-97.
- [10] C. Unluer, A. Al-Tabbaa, Enhancing the carbonation of MgO cement porous blocks through improved curing conditions, Cement and Concrete Research, 59, 2014, 55-65.
- [11] A. Al-Tabbaa, Reactive magnesia cement, in: F. PachecoTorgal, S. Jalali, J. Labrincha, V.M. John (Eds.) Eco-Efficient Concrete, 2013, pp. 523-543.

477 [12] F. Jin, A. Al-Tabbaa, Characterisation of different commercial reactive magnesia,
 478 Advances in Cement Research, 26, 2014, 101-113.

479 [13] Y. Soong, A.L. Goodman, J.R. McCarthy-Jones, J.P. Baltrus, Experimental and
 480 simulation studies on mineral trapping of CO₂ with brine, Energy Conversion and
 481 Management, 45, 2004, 1845-1859.

482 [14] M.L. Druckenmiller, M.M. Maroto-Valer, Carbon sequestration using brine of adjusted
 483 pH to form mineral carbonates, Fuel Processing Technology, 86, 2005, 1599-1614.

484 [15] R. Hao, Investigation into the Production of Carbonates and Oxides from Synthetic
 485 Brine through Carbon Sequestration, in: Department of Engineering, University of
 486 Cambridge, 2017.

487 [16] R. Friedrich, H. Robinson, R. Spencer, Magnesium hydroxide from sea water, in,
 488 Google Patents, 1946.

489 [17] N. Petric, V. Martinac, M. Labor, The effect of mannitol and pH of the solution on the
 490 properties of sintered magnesium oxide obtained from sea water, Chemical Engineering &
 491 Technology, 20, 1997, 36-39.

492 [18] M. Turek, W. Gnot, Precipitation of magnesium hydroxide from brine, Industrial &
 493 Engineering Chemistry Research, 34, 1995, 244-250.

494 [19] R.H. Dave, P.K. Ghosh, Enrichment of bromine in sea-bittern with recovery of other
 495 marine chemicals, Industrial & Engineering Chemistry Research, 44, 2005, 2903-2907.

496 [20] M.H. El-Naas, Reject brine management, in: Desalination, trends and technologies,
 497 InTech, 2011, pp. 237-252.

498 [21] K.T. Tran, T. Van Luong, J.W. An, D.J. Kang, M.J. Kim, T. Tran, Recovery of
 499 magnesium from Uyuni salar brine as high purity magnesium oxalate, Hydrometallurgy, 138,
 500 2013, 93-99.

501 [22] T. Khuyen Thi, K.S. Han, S.J. Kim, M.J. Kim, T. Tam, Recovery of magnesium from
502 Uyuni solar brine as hydrated magnesium carbonate, *Hydrometallurgy*, 160, 2016, 106-114.

503 [23] S. Casas, C. Aladjem, E. Larrotcha, O. Gibert, C. Valderrama, J.L. Cortina, Valorisation
504 of Ca and Mg by-products from mining and seawater desalination brines for water treatment
505 applications, *Journal of Chemical Technology and Biotechnology*, 89, 2014, 872-883.

506 [24] W.R. Eubank, Calcination studies of magnesium oxides, *Journal of the American*
507 *Ceramic Society*, 34, 1951, 225-229.

508 [25] J. Green, Calcination of precipitated Mg (OH) ₂ to active MgO in the production of
509 refractory and chemical grade MgO, *Journal of Materials Science*, 18, 1983, 637-651.

510 [26] K. Itatani, K. Koizumi, F.S. Howell, A. Kishioka, M. Kinoshita, Agglomeration of
511 magnesium oxide particles formed by the decomposition of magnesium hydroxide .1.
512 Agglomeration at increasing temperature, *Journal of Materials Science*, 23, 1988, 3405-3412.

513 [27] V. Choudhary, V. Rane, R. Gadre, Influence of precursors used in preparation of MgO
514 on its surface properties and catalytic activity in oxidative coupling of methane, *Journal of*
515 *Catalysis*, 145, 1994, 300-311.

516 [28] E. Alvarado, L.M. Torres-Martinez, A.F. Fuentes, P. Quintana, Preparation and
517 characterization of MgO powders obtained from different magnesium salts and the mineral
518 dolomite, *Polyhedron*, 19, 2000, 2345-2351.

519 [29] I.F. Mironyuk, V.M. Gun'ko, M.O. Povazhnyak, V.I. Zarko, V.M. Chelyadin, R.
520 Leboda, J. Skubiszewska-Zięba, W. Janusz, Magnesia formed on calcination of Mg(OH)₂
521 prepared from natural bischofite, *Applied Surface Science*, 252, 2006, 4071-4082.

522 [30] L.W. Mo, M. Deng, M.S. Tang, Effects of calcination condition on expansion property
523 of MgO-type expansive agent used in cement-based materials, *Cement and Concrete*
524 *Research*, 40, 2010, 437-446.

525 [31] H. Dong, C. Unluer, E.-H. Yang, A. Al-Tabbaa, Synthesis of reactive MgO from reject
526 brine via the addition of NH_4OH , *Hydrometallurgy*, 169, 2017, 165-172.

527 [32] J.K. Bartley, C. Xu, R. Lloyd, D.I. Enache, D.W. Knight, G.J. Hutchings, Simple
528 method to synthesize high surface area magnesium oxide and its use as a heterogeneous base
529 catalyst, *Applied Catalysis B: Environmental*, 128, 2012, 31-38.

530 [33] L.F. Greenlee, D.F. Lawler, B.D. Freeman, B. Marrot, P. Moulin, Reverse osmosis
531 desalination: water sources, technology, and today's challenges, *Water research*, 43, 2009,
532 2317-2348.

533 [34] C. Fritzmann, J. Lowenberg, T. Wintgens, T. Melin, State-of-the-art of reverse osmosis
534 desalination, *Desalination*, 216, 2007, 1-76.

535 [35] ST, Fifth Singapore desalination plant in the pipeline, in, *The Straits Times*, *The Straits*
536 *Times*, 2016.

537 [36] IDA, The current state of desalination, in, *International Desalination Association*, 2015.

538 [37] S. Adham, A. Hussain, J.M. Matar, R. Does, A. Janson, Application of Membrane
539 Distillation for desalting brines from thermal desalination plants, *Desalination*, 314, 2013,
540 101-108.

541 [38] A.M.O. Mohamed, M. Maraqa, J. Al Handhaly, Impact of land disposal of reject brine
542 from desalination plants on soil and groundwater, *Desalination*, 182, 2005, 411-433.

543 [39] M.H. El-Naas, A.H. Al-Marzouqi, O. Chaalal, A combined approach for the
544 management of desalination reject brine and capture of CO_2 , *Desalination*, 251, 2010, 70-74.

545 [40] D.H. Kim, A review of desalting process techniques and economic analysis of the
546 recovery of salts from retentates, *Desalination*, 270, 2011, 1-8.

547 [41] M. Elimelech, W.A. Phillip, The Future of Seawater Desalination: Energy, Technology,
548 and the Environment, *Science*, 333, 2011, 712-717.

549 [42] L.G. Sillen, A.E. Martell, J. Bjerrum, Stability constants of metal-ion complexes,
550 Chemical Society London, 1964.

551 [43] R.A. Berner, The role of magnesium in the crystal growth of calcite and aragonite from
552 sea water, *Geochimica et Cosmochimica Acta*, 39, 1975, 489-504.

553 [44] T.G. Venkatesha, R. Viswanatha, Y.A. Nayaka, B.K. Chethana, Kinetics and
554 thermodynamics of reactive and vat dyes adsorption on MgO nanoparticles, *Chemical*
555 *Engineering Journal*, 198, 2012, 1-10.

556 [45] C.G. Kontoyannis, N.V. Vagenas, Calcium carbonate phase analysis using XRD and FT-
557 Raman spectroscopy, *The Analyst*, 125, 2000, 251-255.

558 [46] Y. Fukushima, Caustic soda prices on upward trend in Asian markets, 2016.

559 [47] A. Jones, Why do ammonia prices keep falling?, 2016.

560 [48] USGS, Minerals yearbook-lime 2012, 2012.

561 [49] EMA, Singapore energy statistics 2016, Energy Market Authority, 2016.

562 [50] S. Bogner, MGX minerals plans to enter the magnesium market in 2016, Rockstone
563 Reserach Ltd., 2015.

564